JACS
JOURNAL OF THE AMERICAN CHEMICAL SOCIETY
Article
pubs.acs.org/JACS

Captodatively Stabilized Biradicaloids as Chromophores for Singlet Fission

Jin Wen,[†] Zdeněk Havlas,[†] and Josef Michl*[,†,‡]

[†]Institute of Organic Chemistry and Biochemistry, Academy of Sciences of the Czech Republic, Flemingovo nám. 2, 16110 Prague 6, Czech Republic

[‡]Department of Chemistry and Biochemistry, University of Colorado, Boulder, Colorado 80309-0215, United States

Supporting Information

ABSTRACT: Singlet fission offers an opportunity to improve solar cell efficiency, but its practical use is hindered by the limited number of known efficient materials. We look for chromophores that satisfy the desirable but rarely encountered adiabatic energy conditions, $E(T_2) - E(S_0) > E(S_1) - E(S_0) \approx 2[E(T_1) - E(S_0)]$, and are small enough to permit highly accurate calculations. We provide a rationale for the use of captodative biradicaloids, i.e., biradicals stabilized by direct interaction between their radical centers, which carry both an acceptor and a donor group. A computation of vertical excitation energies of 14 structures of this type by time-dependent density functional theory (TD-DFT) yielded 11 promising candidates. The vertical excitation energies from S_0 and T_1 were recalculated by complete-active-space second-order perturbation theory (CASPT2), and five of the compounds met the above energy criteria. Their adiabatic excitation energies from the S_0 into the S_1, S_2, T_1, and T_2 excited states were subsequently calculated, and three of them look promising. For 2,3-diamino-1,4-benzoquinone, adiabatic $E(T_1)$ and $E(S_1)$ energies were close to optimal (1.12 and 2.23 eV above the S_0 ground state, respectively), and for its more practical *N*-peralkylated derivative they were even lower (0.63 and 1.06 eV above S_0, respectively). PCM/CASPT2 results suggested that the relative energies can be further tuned by varying the polarity of the environment.

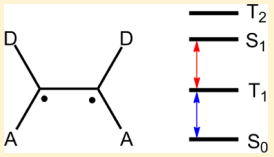

INTRODUCTION

Singlet fission is a process in which a singlet excited chromophore transfers some of its excitation energy to a ground-state neighbor and both end up in their excited triplet states.[1,2] The triplets are coupled into an overall singlet, making this conversion of singlet into triplet states spin-allowed and potentially very fast. Its exploitation in a solar cell could lead to a significant increase in maximum theoretical efficiency,[3] and this prospect has produced a recent surge of activity.

One of the main problems that need to be overcome if singlet fission solar cells are to become practical is the tiny number of materials in which singlet fission is fast enough to outcompete all other processes that depopulate the singlet excited state, and which thus produce triplets in a quantum yield close to 200%. Simultaneously, mutual annihilation of the resulting triplets needs to be slow enough not to compete with their use for charge separation. The problem can be approached by searching for structures in which the rate of singlet fission is intentionally maximized and those of all competing monomolecular and bimolecular processes minimized.

In an effort to uncover additional materials that perform singlet fission efficiently, three immediate tasks need to be addressed.[1,2]

(i) Identification of chromophores whose first singlet excitation energy $E(S_1) - E(S_0)$ lies within ~0.1−0.2 eV of twice the first triplet excitation energy $E(T_1) - E(S_0)$, and in which the second triplet excitation energy $E(T_2) - E(S_0)$ is higher than $2[E(T_1) - E(S_0)]$, making T_1−T_1 annihilation to yield T_2 endothermic and slow. (Annihilation to yield S_1 does not represent an energy loss, although it is still obviously kinetically disadvantageous, annihilation to the lowest quintet Q_1 is energetically prohibitive, and annihilation to S_0 or T_1 is slow according to the energy-gap law.)[4] Ultimately, to maximize the singlet fission rate, minor structural adjustments may be needed to fine-tune the process to optimal slight exothermicity.[5−7] The chromophores should not undergo any photophysical or photochemical processes that might compete with singlet fission; i.e., in isolation they should have a fluorescence quantum yield close to unity.

(ii) Identification of an optimal geometry for interchromophore coupling in the singlet fission process in a crystal, aggregate, oligomer, or dimer structure. This geometry should also minimize the rates of competing intermolecular deactivation processes, for instance excimer formation and charge separation. At the same time, intermolecular interactions such as Davydov splitting should not modify the desirable energy level relations $E(T_2) - E(S_0) > E(S_1) - E(S_0) \approx 2[E(T_1) - E(S_0)]$ established in an isolated chromophore.

(iii) Finally, identification of conditions that will ensure full utilization of both triplets for charge separation. This requires a minimization of the quenching of the second triplet by spin one-half polarons (radical cation and radical anion) that result from charge separation performed by the first triplet. It is less of an issue in solids, in which the two triplets can diffuse far apart

Received: July 11, 2014
Published: December 5, 2014

   dx.doi.org/10.1021/ja5070476 | J. Am. Chem. Soc. 2015, 137, 165−172

and become independent, than it is in aggregates, oligomers, or dimers, in which they cannot.

In the present study, we only tackle the first of the three tasks, in a fashion that is similar in spirit to our earlier work[4,8] and to a recent effort by another research group.[9] We have two goals in mind. On the one hand, we hope to find a chromophore whose molecules are small enough for a thorough high-quality quantum chemical and dynamical treatment of a dimer or higher aggregate, since the currently most popular choices, tetracene and pentacene, are too large. On the other hand, we are looking for a material that absorbs everywhere above about 2.2 eV and is sturdy enough to survive long-term exposure to solar radiation. It would be best if both goals could be met in the same structure simultaneously, but it is not necessary.

RESULTS

Biradicaloids for Singlet Fission. The class of chromophores selected for our study are biradicaloids, one of the two partly overlapping classes identified some time ago by a simple theoretical consideration[4] and later elaborated in more detail[10,11] using concepts and formulations first introduced in the 3 × 3 model of biradical electronic structure.[12−16] This model is very crude but has considerable heuristic value.

In a perfect biradical, S_0 and T_1 are close in energy, and the other two states resulting from an intra-shell excitation, S_1 and S_2, lie higher. When a covalent perturbation[14,16] is introduced, S_0 is stabilized, while the T_1 state and usually also the S_1 state are destabilized. It follows that there is a range of perturbation strengths at which $E(S_1) - E(S_0) \approx 2[E(T_1) - E(S_0)]$. At the same time, there is a good chance that T_2, which originates from an inter-shell excitation, will lie above S_1. A simple illustration is provided in Figure 1, which shows the effect of covalent perturbation on the S_0, T_1, and S_1 valence-state energies of two perfect biradicals, a separated pair of hydrogen atoms and an orthogonally twisted ethylene,[17] and demonstrates how the optimal state energy relations can be induced by a covalent perturbation of a perfect biradical. The perturbation is introduced in the former by providing σ overlap of the orbitals at the two radical centers, and in the latter by providing π overlap. In the case of ethylene (Figure 1B), the situation is complicated by the presence of Rydberg states, and even full planarization is not quite sufficient to make $E(S_1) - E(S_0)$ equal to $E(T_1) - E(S_0)$, but the general trend is apparent.

When dealing with isolable species in the laboratory, structural changes can be introduced into a molecule in small steps but not in a fully continuous manner. A recipe for finding a suitable singlet fission chromophore then is to identify a perfect biradical and to perturb it covalently in the direction of producing an ordinary closed-shell ground state molecule, not too little and not too much. This approach was used to derive the first structure specifically designed for efficient singlet fission, 1,3-diphenylisobenzofuran.[4,18−21] It has also been used to comprehend why indigo[22] and its simple derivative, cibalackrot,[23] satisfy the condition $E(S_1) - E(S_0) \approx 2[E(T_1) - E(S_0)]$. A small mesoionic heterocycle identified by this procedure has been proposed as a good prospect for singlet fission[8] but to our knowledge has not been synthesized.

The 3 × 3 Model for Biradicaloids. In the simple 3 × 3 (two-electron, two-orbital) model of biradicaloid electronic structure,[14,16] a quantitative formulation of the problem is easy and heuristically instructive. The functional space in this model

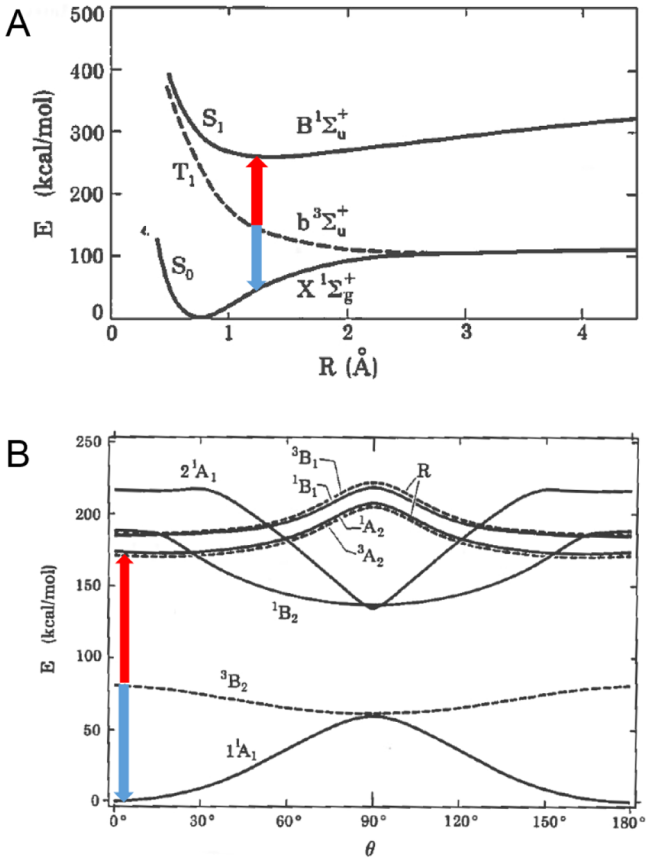

Figure 1. Computed potential energy curves of low-energy states of H_2 (A) and ethylene (B), as a function of internuclear separation R and of twist angle θ, respectively. Rydberg states of ethylene are indicated by letter R. Reproduced with permission from ref 17. Copyright 1990 John Wiley and Sons, Inc.

spans only the S_0, S_1, and S_2 singlet states and the three components of the T_1 triplet state. In terms of the most localized orthogonal form of the two orbitals, A and B, the six wave functions describing these states for a perfect biradical (A and B degenerate) are $S[u]\Sigma$ for the three singlets and $T\Theta[u]$ for the three components of the triplet ($u = x, y, z$), and

$$S[x] \text{ or } \Theta[x] = -2^{-1/2}[a(1)a(2) - b(1)b(2)]$$

$$S[y] \text{ or } \Theta[y] = i2^{-1/2}[a(1)a(2) + b(1)b(2)]$$

$$S[z] \text{ or } \Theta[z] = -2^{-1/2}[a(1)b(2) - b(1)a(2)]$$

where for S and T, a = A, b = B, and for Σ and Θ, $a = \alpha$, $b = \beta$ (the choice of the phase factors assures cyclic permutation properties with respect to x, y, and z). The molecular axes x, y, and z are the principal axes of the spin−spin dipolar coupling tensor, and spin−orbit coupling is neglected. Relative to the average energy of the T_1 sublevels, $E(T_1) = h_A + h_B + J_{AB} - K_{AB}$, the energies of the S_0 ($S[z]\Sigma$), S_1 ($S[x]\Sigma$), and S_2 ($S[y]\Sigma$) states of a perfect biradical are $2K_{AB}$, $2K'_{AB}$, and $2(K_{AB} + K'_{AB})$. Here, h_A and h_B are the diagonal matrix elements of the one-electron part of the Hamiltonian, i.e., one-electron energies of A and B, respectively, K_{AB} is the exchange integral between A and B, and K'_{AB} is the exchange integral between the most delocalized real orbitals $2^{-1/2}$(A + B) and $2^{-1/2}$(A − B), which can also be written as $K'_{AB} = [(J_{AA} + J_{BB})/2 - J_{AB}]/2$, where J_{AA}, J_{BB}, and J_{AB} are Coulomb repulsion integrals.

dx.doi.org/10.1021/ja5070476 | J. Am. Chem. Soc. 2015, 137, 165−172

Chart 1. Chemical Structures 1−14

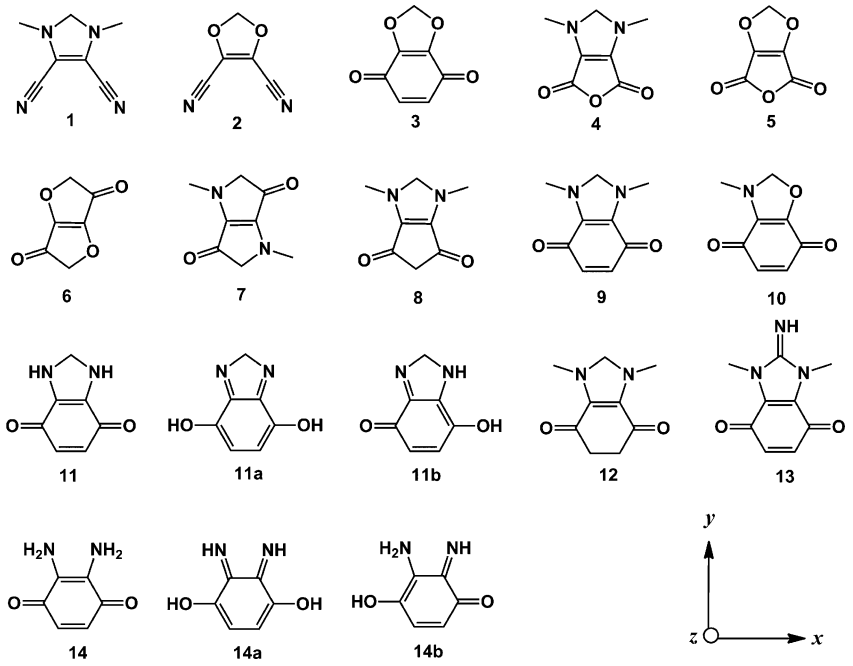

A perfect biradical can be perturbed by outside fields or by structural changes in three linearly independent ways (polarizing, magnetizing, and covalent), which mix the three zero-order states. Only the covalent perturbation is of interest presently.[14,16] Its strength is described by the matrix element γ_{AB}, which mixes the S_0 and S_2 states of the perfect biradical and is approximately equal to twice the resonance integral β_{AB} of semiempirical theories. It can be viewed as a measure of the strength of covalent interaction between orbitals A and B and is defined as $\gamma_{AB} = 2h_{AB} + (AA|AB) + (BB|BA)$, where h_{AB} is the matrix element of the one-electron part of the Hamiltonian between orbitals A and B, and (AA|AB) and (BB|BA) are hybrid repulsion integrals.

It is readily seen that in this model the strength of the covalent perturbation γ_{AB} that is required to make the energy difference $E(S_1) - E(S_0)$ equal to twice the energy difference $E(T_1) - E(S_0)$ is given by $|\gamma_{AB}|_{crit} = 2[(K'_{AB} + K_{AB})(2K'_{AB} + K_{AB})]^{1/2}$, and this formula provides a useful starting guideline (cf. Table S6 in Supporting Information). For example, in agreement with the ab initio results shown in Figure 1, for ethylene this simple model suggests that complete planarization is needed for γ to reach the critical value $|\gamma_{AB}|_{crit}$: taking $K_{AB} = 0$ from the zero-differential-overlap (ZDO) approximation and the range $K'_{AB} = (J_{AA} - J_{AB})/2 = 1.7-2.5$ eV from one or another parametrization of the Pariser−Parr−Pople (PPP) model,[4] we obtain $|\gamma_{AB}|_{crit}/2 = 2.4-3.5$ eV, and a typically used value of the resonance integral β_{AB} in ethylene is ∼2.5 eV.

Initial Guesses for Optimal Biradicaloids. We focus on planar π-electron systems, which are likely to have high extinction coefficients, preferentially throughout the visible region. We describe the above qualitative argument in more detail and use it to identify 14 initial biradicaloid test structures that appear worthy of examination.

In the first step, we envisage a hypothetical perfect biradical[14,16] that does not need to be physically realizable. We start with an arbitrarily chosen planar conjugated system and select a valence-bond structure with two isolated atomic centers carrying single electrons. We then construct a perfect biradical on paper by suppressing all conjugation between the two selected radical centers by the installation of formal insulating walls across appropriate bonds. Computationally, this is readily represented at the level of the Hückel molecular orbital theory (HMO) or of the natural bonding orbital theory (NBO),[24] where the introduction of insulating walls is achieved by the deletion of matrix elements of the Hückel or Fock operators between atomic centers, respectively. At the present heuristic level of argument, no computation is actually necessary.

In the second step, the insulating walls in the hypothetical structure are again removed, i.e., the deleted matrix elements are reintroduced and the original structure recovered. This represents the perturbation necessary to proceed toward a biradicaloid in which the condition $E(S_1) - E(S_0) \approx 2[E(T_1) - E(S_0)]$ is hopefully fulfilled. Whether in the resulting real molecule this point is not quite reached, $E(S_1) - E(S_0) > 2[E(T_1) - E(S_0)]$, just attained, $E(S_1) - E(S_0) = 2[E(T_1) - E(S_0)]$, or overshot, $E(S_1) - E(S_0) < 2[E(T_1) - E(S_0)]$, depends on its detailed structure, and this is where the guidance obtained from the simple formula for $|\gamma_{AB}|_{crit}$ can be useful. In a small conjugated hydrocarbon, the removal of the wall that prevents the direct interaction of the two radical centers will often stabilize the S_0 state too much, but the degree of stabilization will be reduced if the structure is suitably modified. The structure can be adjusted in a way that makes the perturbation of the perfect biradicaloid weaker or stronger, as required. At the same time an adjustment of the $E(S_1) - E(S_0)$ gap toward the optimal value of 2.2 eV can be attempted by stabilization of the two radical centers. The modifications introduced at this stage lead to new structures related to the initial one, but not quite identical.

Since we are looking for the smallest possible chromophores, we have presently chosen ethylene as the initial structure. In a general case of a starting system other than ethylene, especially much larger systems, one could use the semiempirical PPP theory to ascertain rapidly whether the desired value of $|\gamma_{AB}|_{crit}$ has been reached, which is what in effect was done in ref 4.

dx.doi.org/10.1021/ja5070476 | J. Am. Chem. Soc. 2015, 137, 165−172

There, attention was paid to differences between the equilibrium geometries in the various electronic states, and we believe that this is important in general. This argues against the use of even simpler approaches, such as the 3 × 3 model itself.

The introduction of an insulating wall between its carbons of ethylene produces a pair of non-interacting carbon $2p_z$ orbitals as a perfect biradical. We then stabilize them by removal of the insulating wall. If only valence states are considered, Figure 1 and the simple qualitative argument given above both suggest that the resulting planar double bond chromophore is not quite stabilized enough to satisfy the energy relation $E(S_1) - E(S_0) = 2[E(T_1) - E(S_0)]$ that we are looking for, but that it comes close, with $E(T_1) - E(S_0)$ a little too small. Ethylene absorption occurs at energies that are much too high for use in solar cells, yet it might nevertheless be interesting for fundamental studies if complications introduced by the presence of low-energy Rydberg excitations could be suppressed by going to the condensed phase.

Since the desired energy relation between S_0, T_1, and S_1 already is approximately satisfied in planar ethylene, our task is reduced to decreasing $E(S_1) - E(S_0)$ by a suitable perturbation of the hypothetical starting perfect biradical without increasing its size significantly. We examine a particular case in which the interaction between the radical centers is diminished by simultaneous attachment of a donor and an acceptor substituent to each. This type of radical stabilizing substitution is commonly referred to as captodative. It was first observed in the stable *N*-methyldihydropyridine-4-carbethoxy radical half a century ago,[25] and its generality was soon recognized.[26,27] A definitive review is available.[28]

Experience with indigo suggests that captodative substitution at both ethylene carbons with amino and carbonyl groups will reduce the $E(S_1) - E(S_0)$ gap to a degree that is about right, but we have experimented with other substituents as well: cyano for an acceptor, and an ether oxygen as a weaker donor. The addition of various other structural elements then led to the 14 test structures listed in Chart 1 (likely tautomers of **11** and **14** are shown as well).

The mechanism by which captodative substitution reduces the HOMO−LUMO gap in ethylene is easily understood using an HMO model (Figure 2). The argument is particularly simple if the donor strength and the acceptor strength are equal. In energy units of the (negative) resonance integral β (assumed to be the same for all bonds), and with the energy of an electron in a non-interacting $2p_z$ AO on carbon defined as zero, in an unsubstituted ethylene the interaction of the AOs on the two centers produces a HOMO energy of 1 and a LUMO energy of −1. After the addition of a donor and an acceptor at each center, the two starting $2p_z$ orbitals are replaced with two allyl-like systems whose MOs interact through their central atoms only. In each one, one of the terminal AOs is a donor with a doubly occupied orbital at energy d and the other is an acceptor with a vacant orbital at energy $-d$, $0 < d < \infty$. Each of the two allyl-like systems will then have a bonding MO at energy $(2 + d^2)^{1/2}$, an antibonding MO at energy $-(2 + d^2)^{1/2}$, and a non-bonding MO at energy 0 that is bonding between the acceptor and the central atom and antibonding between the donor and the central atom, with coefficients $c_D = -(2 + d^2)^{-1/2}$ at the donor AO, $c = d(2 + d^2)^{-1/2}$ at the central AO, and $c_A = (2 + d^2)^{-1/2}$ at the acceptor AO.

The interaction of the non-bonding MOs on the two partners will produce the HOMO and the LUMO of the captodatively perturbed ethylene. To first order, the HOMO will be stabilized by an amount equal to the effective resonance integral of the new bond and the LUMO will be destabilized by the same amount. The effective resonance integral is the bond resonance integral β multiplied by the AO expansion coefficients of the two interacting MOs at their interacting centers. These were unity in the unsubstituted ethylene, but in the case of two identical allyl-like systems each equals $d(2 + d^2)^{-1/2}$ and the effective resonance integral is $d^2(2 + d^2)^{-1}$, which is less than unity. Instead of a HOMO−LUMO gap of 2 in the unperturbed ethylene, the captodative system will have a gap of only $2d^2(2 + d^2)^{-1}$. As the donor and acceptor abilities of the donor and the acceptor grow and d approaches zero, so does the gap. As these abilities diminish and d approaches infinity, the gap approaches 2.

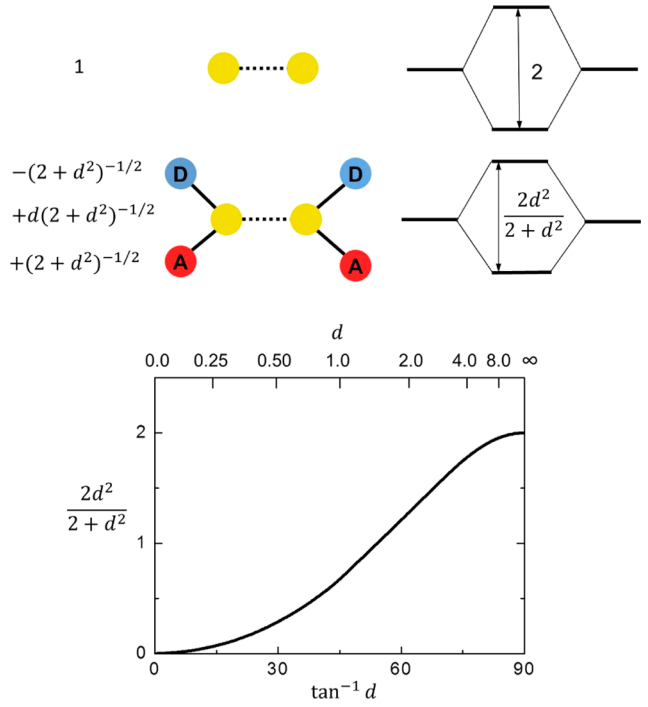

Figure 2. First-order Hückel model for the effect of captodative substitution on the HOMO−LUMO gap in ethylene. Left, coefficients on AOs in the MOs of the interacting fragments. Right, MO energies. The energies of the occupied donor (D) and unoccupied acceptor (A) AOs are $+d$ and $-d$, respectively, in units of the (negative) resonance (hopping) integral.

TD-DFT Evaluation of Vertical Excitation Energies. In order to determine which of the candidates **1**−**14** are likely to satisfy the conditions $E(T_2) - E(S_0) > E(S_1) - E(S_0) \approx 2[E(T_1) - E(S_0)]$, we need a relatively fast yet fairly reliable method. We could have chosen the PPP method but decided in favor of a time-dependent density functional (TD-DFT) procedure with a long-range corrected functional, CAM-B3LYP, suitable for compounds with charge-transfer states.[29] For biradicaloids, this method gives fairly accurate excitation energies within the singlet and triplet manifolds, but higher level calculations reveal that the energies of the triplets are too low relative to those of the singlets.[30] As a result, the condition $E(S_1) - E(S_0) \geq 2[E(T_1) - E(S_0)]$ tends to be satisfied by the TD-DFT energies too easily and the method tends to yield false positives. However, structures that do not satisfy this condition at the TD-DFT level can be safely discarded as unsuitable.

dx.doi.org/10.1021/ja5070476 | J. Am. Chem. Soc. 2015, 137, 165−172

Table 1. CASPT2/ANO-L-VTZP Vertical Excitation Energies (E in eV), Oscillator Strengths (f), and Polarizations at S_0 Equilibrium Geometry (see Chart 1)[a]

	1	2	3	7	8	9	10	11	12	13	14
S_1	3.49	4.40	2.67	2.34	2.86	1.50	2.54	2.03	2.82	1.71	2.63
S_2	5.28	5.19	2.82	3.17	3.26	2.70	2.91	2.91	3.65	5.48	2.76
T_1	2.40	2.67	2.15	2.00	2.25	1.41	1.81	1.67	2.17	1.38	1.89
T_2	5.63	4.96	2.65	3.09	3.11	2.51	3.22	2.71	3.52	3.06	2.97
f (S_0–S_1)	0.18(x)	0.20(x)	0.03(x)	0.15(x)	0.16(x)	0.02(x)	0.06(x)	0.05(x)	0.20(x)	0.03(x)	0.05(x)
f (S_0–S_2)	0.11(x)	0.00	0.00	0.00	0.00	0.00	0.00	0.02(y)	0.06(y)	0.00	0.35(x)
f (S_1–S_2)	0.06(y)	0.00	0.01(x)	0.00	0.00	0.00	0.00	0.00	0.00	0.06(x)	0.08(y)
f (T_1–T_2)	0.01(x)	0.00	0.00	0.00	0.00	0.00	0.00	0.00	0.05(y)	0.00	0.00

[a]For the most stable conformer (**9** and **11**, C_s; **14**, C_2).

Table 2. CASPT2/ANO-L-VTZP Adiabatic Excitation Energies (E in eV, No Solvent), Dipole Moments (μ in Debye, from Positive to Negative End), and Difference in Dipole Moments Relative to the S_0 State ($\Delta\mu$ in Debye)[a]

	2			8			9			11			14		
	E	μ	$\Delta\mu$	E	μ	$\Delta\mu$	E	μ	$\Delta\mu$	E	μ	$\Delta\mu$	E	μ	$\Delta\mu$
S_0	0.00	5.27		0.00	3.40		0.00	1.93		0.00	2.25		0.00	0.25	
S_1	4.18	8.77	3.50	2.57	8.99	5.76	1.06	8.46	7.31	1.36	7.33	6.46	2.23	5.25	5.00
S_2	4.64	7.88	2.61	2.88	3.18	0.29	2.60	6.88	5.86	2.30	5.56	5.08	2.59	4.19	3.94
T_1	2.26	6.41	1.14	1.77	6.54	3.38	0.63	6.22	5.13	0.67	6.52	5.65	1.12	4.75	4.50
T_2	4.30	6.78	1.51	2.77	3.08	0.44	2.21	8.53	7.40	2.43	2.41	0.15	2.74	0.52	0.26

[a]For the most stable conformer (**9** and **11**, C_s; **14**, C_2).

The TD-DFT CAM-B3LYP/TZVP vertical excitation energies of compounds **1**–**14** evaluated at CAM-B3LYP/TZVP-optimized geometries are listed in Table S4 (Supporting Information). The calculated intensities of the S_0 to S_1 transitions appear adequate for use in singlet fission, but only compounds **1**–**3** and **7**–**14** meet the condition $E(S_1) - E(S_0) \geq 2[E(T_1) - E(S_0)]$. The other structures need not be considered further.

CASPT2 Evaluation of Vertical and Adiabatic Excitation Energies. In the next round of elimination, we used the CASPT2/ANO-L-VTZP method at CASPT2/ANO-S-VDZP-optimized geometries to obtain more accurate vertical excitation energies of the remaining compounds (Table 1). The results permitted us to eliminate most of the candidates and to focus on compounds **2**, **8**, **9**, **11**, and **14**. For these, we have evaluated CASPT2/ANO-L-VTZP adiabatic excitation energies (Table 2). The natural orbitals that characterize the active space used in these calculations are shown in the Supporting Information (Figures S1–S5). Table 2 shows that only compounds **9**, **11**, and **14** are predicted to meet the adiabatic conditions $E(T_2) - E(S_0) > E(S_1) - E(S_0) \approx 2[E(T_1) - E(S_0)]$. Figures 3–7 provide a description of the nature of the low-lying electronic states. They, and Tables 1 and 2, show that the nature of the important MOs and states, and also the trends in their energies as a function of donor and acceptor strength, fit very well the expectations based on the simple model description provided above (cf., for instance, the trend in excitation energies in the series **14**, **11**, **9**, as the donor strength of the amino groups is gradually enhanced by alkylation).

The symmetries of the ground and excited states are lower than might be expected, because the amino groups are pyramidalized. In isolated molecules **9** and **11**, the C_s form is calculated to be more stable than the C_2 form by 4.3 and 3.2 kcal/mol, respectively, whereas in isolated **14**, it is calculated to be less stable by 2.1 kcal/mol. The various forms differ slightly in their adiabatic excitation energies to the S_1 and T_1 states (Supporting Information).

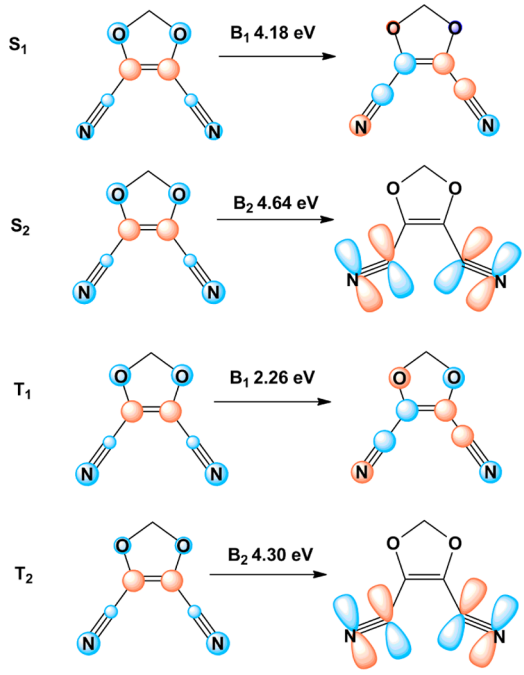

Figure 3. Dominant electron promotions in low-lying states of **2** (C_{2v}) with adiabatic excitation energies.

Another possible complication is the formation of tautomers of **11** and **14** (Chart 1). In the gas phase at the CAM-B3LYP/TZVP level, **11a** is 3.6 kcal/mol more stable and **11b** is 6.5 kcal/mol less stable than **11**, while both **14a** and **14b** are considerably less stable than **14**, by 21.9 and 14.1 kcal/mol, respectively (for their CASPT2 excitation energies, see Table S5).

The large difference between the vertical and adiabatic T_1 excitation energies, especially for **14**, are associated with considerable changes in C–O and C–N bond lengths. In the

dx.doi.org/10.1021/ja5070476 | J. Am. Chem. Soc. 2015, 137, 165–172

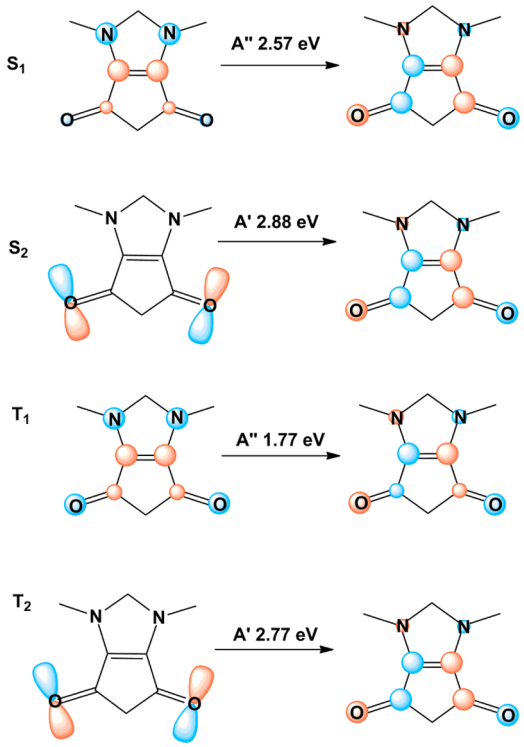

Figure 4. Dominant electron promotions in low-lying states of **8** (C_s) with adiabatic excitation energies.

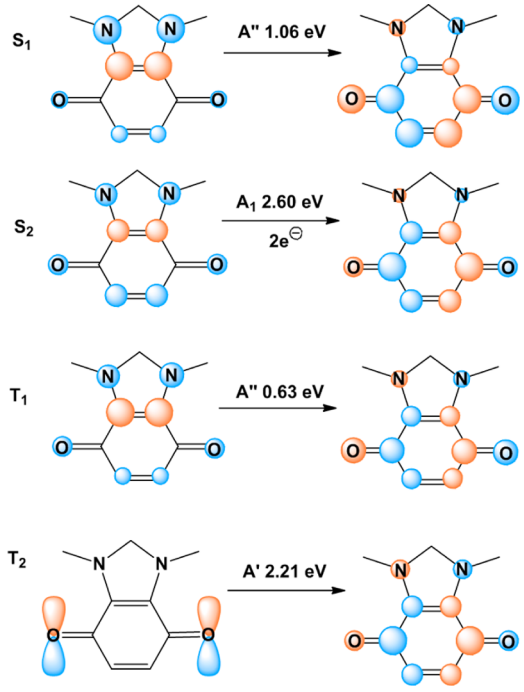

Figure 5. Dominant electron promotions in low-lying states of **9** (C_s, C_{2v} for the S_2 state) with adiabatic excitation energies. The symbol $2e^{\ominus}$ indicates a dominant doubly excited configuration.

excited state, the C−O distance increases and the C−N distance is reduced, as would be expected from a charge-transfer transition in which an electron is moved from a mainly C−N antibonding MO to a mainly C−O antibonding MO.

Solvent Effects. Because of the charge-transfer nature of many of the computed transitions, one can expect that the polarity of the environment will have a significant effect on the excitation energies. We have examined this for structure **14** using the PCM-CASPT2/ANO-L-VTZP method (Table 3) and found that the excitation energies of the charge-transfer transitions into the S_1 and T_1 states decrease as solvent polarity increases, while the excitation energies of the S_2 and T_2 are unaffected.

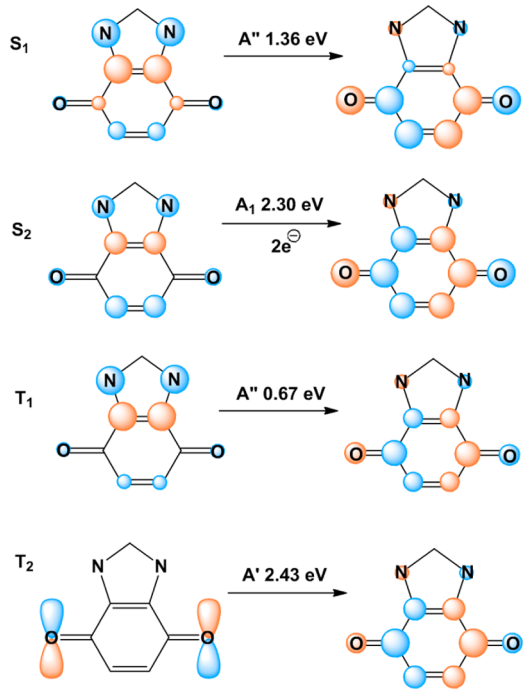

Figure 6. Dominant electron promotions in low-lying states of **11** (C_s, C_{2v} for the S_2 state) with adiabatic excitation energies. The symbol $2e^{\ominus}$ indicates a dominant doubly excited configuration.

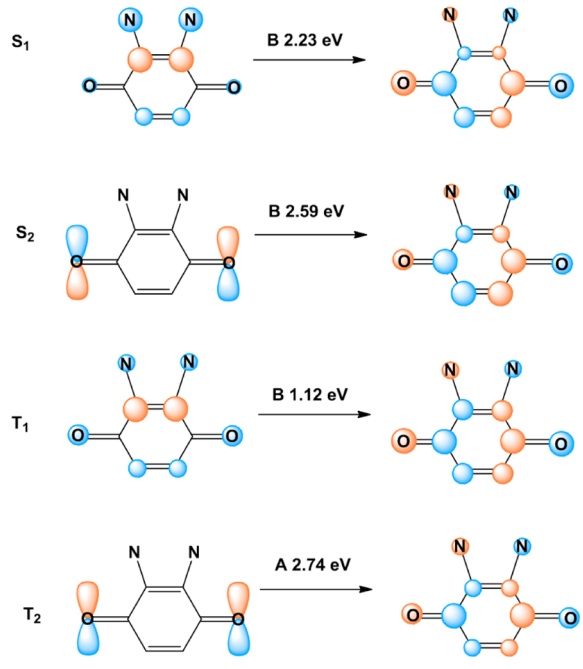

Figure 7. Dominant electron promotions in low-lying states of **14** (C_2) with adiabatic excitation energies.

dx.doi.org/10.1021/ja5070476 | J. Am. Chem. Soc. 2015, 137, 165−172

Table 3. PCM-CASPT2/ANO-L-VTZP Adiabatic Excitation Energies of 14 at Gas-Phase C_2 Geometries (in eV) and Solvent Dielectric Constants (ε)

	benzene (ε = 2.25)	THF (ε = 7.58)	DMSO (ε = 46.70)
S_1	2.22	2.06	1.98
S_2	2.68	2.74	2.74
T_1	1.03	0.85	0.76
T_2	2.76	2.78	2.79

DISCUSSION AND CONCLUSIONS

The S_0-to-S_1 and S_0-to-T_1 excitations can be characterized as charge-transfer transitions (Figures 3−7) and accordingly involve a large dipole moment change, making the calculated sensitivity to solvent effects (Table 3) understandable.

Judging by the adiabatic excitation energies in Table 1 alone, compounds **9**, **11**, and **14** are of interest for experimental work. Although the small size and simplicity of the structures **11** and **14** are very attractive, and although they may be useful as a source of inspiration, the presence of potentially mobile protons in their NH groups is an invitation for various complications. The molecules could engage in solvent-dependent intramolecular or intermolecular ground-state and excited state hydrogen bonding or even proton transfer, and could prefer to exist as the tautomers **11a**, **11b**, **14a**, and **14b**. Calculations on isolated molecules provide only a very rough guide to the relative stability of tautomers in solutions and solids, but they suggest that **14a** and **14b** are not viable, whereas the possible presence of **11b** and especially **11a** needs to be considered.

In the excited states of **14**, the amino groups could also twist out of plane and open a new deactivation channel. Additional complexity is introduced by the pyramidalization of the two amino groups at the equilibrium geometry. The pyramidalization can take place in the same sense on both nitrogen atoms (C_s), or in the opposite sense (C_2), and the resulting conformers have somewhat different ground-state and excitation energies.

For these reasons, structure **9** is actually the most appealing as a possible subject of an experimental investigation, in spite of its larger size, more involved synthesis, and excessively small excitation energies. Although the T_1 excitation energies of **9** and **11** may be too low for realistic photovoltaic systems unless they can be adjusted by suitable environmental effects, the compounds could still be useful for mechanistic studies.

If potential difficulties with hydrogen bonding, proton transfer and tautomerism, and amino group twisting could be overcome, the diaminoquinone **14** would become the most promising candidate as a singlet fission molecule among all the compounds in Chart 1. With only 10 non-hydrogen atoms, it is far smaller than any of the molecules in which singlet fission is known to be efficient, and thus promising for a detailed investigation. This compound does not appear to be well characterized in the literature, but its synthesis should be easier and its stability higher than those of the only other small molecule suggested earlier.[8]

METHODS OF CALCULATION

DFT calculations were performed with Gaussian 09 Revision A.02.[31] The S_0 geometries of **1**−**14** were optimized using the CAM-B3LYP[32] functional and the TZVP basis set.[33] Vibrational frequency calculations were performed to make sure the optimized structures are true minima. The TD-DFT calculations of vertical excitation energies of singlet and triplet excited states were performed at the same level.

All CASPT2[34,35] calculations here were performed with MOLCAS 7.6,[36−38] using the π orbitals and lone pairs of oxygen or nitrogen atoms in the active space. The ANO-S-VDZP[39] basis set was used initially to optimize S_0 geometries and to obtain vertical excitation energies. The final results were obtained at geometries optimized separately for each state at the CASPT2/ANO-S-VDZP level.[40,41] The symmetry of **9**, **11**, and **14** at the equilibrium geometry in ground and excited states was tested by using unsymmetrically perturbed geometries as starting points for optimizations. Equilibrium geometries in excited states were found to have the same symmetry as in the ground state, except for **9** and **11** in the S_2 state. These two equilibrium structures are of C_s symmetry in their ground state and C_{2v} in the S_2 state.

The cavity-based reaction-field Polarizable Continuum Model (PCM)[42,43] was used to study the solvation effect on the excitation energies at gas-phase optimized geometries.

ASSOCIATED CONTENT

Supporting Information

Lists of the atomic coordinates and absolute energies at optimized geometries, CAM-B3LYP/TZVP vertical excitation energies, CASPT2/ANO-L-VTZP absolute energies, and both vertical and adiabatic excitation energies. Natural orbitals of the active spaces used for **2**, **8**, **9**, **11**, and **14**. This material is available free of charge via the Internet at http://pubs.acs.org.

AUTHOR INFORMATION

Corresponding Author

michl@eefus.colorado.edu

Notes

The authors declare no competing financial interest.

ACKNOWLEDGMENTS

This material is based upon work supported by the U.S. Department of Energy, Office of Basic Energy Sciences, Division of Chemical Sciences, Biosciences, and Geosciences, under award no. DE-SC0007004, and the postdoctoral program of the Institute of Organic Chemistry and Biochemistry, Academy of Sciences of the Czech Republic (RVO: 61388963).

REFERENCES

(1) Smith, M. B.; Michl, J. *Chem. Rev.* **2010**, *110*, 6891.
(2) Smith, M. B.; Michl, J. *Annu. Rev. Phys. Chem.* **2013**, *64*, 361.
(3) Hanna, M.; Nozik, A. J. *J. Appl. Phys.* **2006**, *100*, 074510/1.
(4) Paci, I.; Johnson, J. C.; Chen, X.; Rana, G.; Popović, D.; David, D. E.; Nozik, A. J.; Ratner, M. A.; Michl, J. *J. Am. Chem. Soc.* **2006**, *128*, 16546.
(5) Berkelbach, T. C.; Hybertsen, M. S.; Reichman, D. R. *J. Chem. Phys.* **2013**, *138*, 148103.
(6) Yost, S. R.; Lee, J.; Wilson, M. W. B.; Wu, T.; McMahon, D. P.; Parkhurst, R. R.; Thompson, N. J.; Congreve, D. N.; Rao, A.; Johnson, K.; Sfeir, M. Y.; Bawendi, M. G.; Swager, T. M.; Friend, R. H.; Baldo, M. A.; Van Voorhis, T. *Nat. Chem.* **2014**, *6*, 492.
(7) Busby, E.; Berkelbach, T. C.; Kumar, B.; Chernikov, A.; Zhong, Y.; Hlaing, H.; Zhu, X.-Y.; Heinz, T. F.; Hybertsen, M. S.; Sfeir, M. Y.; Reichman, D. R.; Nuckolls, C.; Yaffe, O. *J. Am. Chem. Soc.* **2014**, *136*, 10654.
(8) Akdag, A.; Havlas, Z.; Michl, J. *J. Am. Chem. Soc.* **2012**, *134*, 14624.
(9) Zeng, T.; Ananth, N.; Hoffmann, R. *J. Am. Chem. Soc.* **2014**, *136*, 12638.
(10) Minami, T.; Nakano, M. *J. Phys. Chem. Lett.* **2012**, *3*, 145.
(11) Nakano, M. *Excitation Energies and Properties of Open-Shell Singlet Molecules*; Springer: New York, 2014.

(12) Salem, L.; Rowland, C. *Angew. Chem., Int. Ed.* **1972**, *11*, 92.
(13) Michl, J. *Mol. Photochem.* **1972**, *4*, 257.
(14) Bonačić-Koutecký, V.; Koutecký, J.; Michl, J. *Angew. Chem., Int. Ed. Engl.* **1987**, *26*, 170.
(15) Michl, J. *J. Mol. Struct. (THEOCHEM)* **1992**, *260*, 299.
(16) Michl, J. *J. Am. Chem. Soc.* **1996**, *118*, 3568.
(17) Michl, J.; Bonačić-Koutecký, V. *Electronic Aspects of Organic Photochemistry*; John Wiley and Sons, Inc.: New York, 1990.
(18) Schwerin, A. F.; Johnson, J. C.; Smith, M. B.; Sreearunothai, P.; Popović, D.; Černý, J.; Havlas, Z.; Paci, I.; Akdag, A.; MacLeod, M. K.; Chen, X.; David, D. E.; Ratner, M. A.; Miller, J. R.; Nozik, A. J.; Michl, J. *J. Phys. Chem. A* **2010**, *114*, 1457.
(19) Johnson, J. C.; Nozik, A. J.; Michl, J. *J. Am. Chem. Soc.* **2010**, *132*, 16302.
(20) Schrauben, J.; Ryerson, J.; Michl, J.; Johnson, J. *J. Am. Chem. Soc.* **2014**, *136*, 7363.
(21) Ryerson, J.; Schrauben, J. N.; Ferguson, A. J.; Sahoo, S. C.; Naumov, P.; Havlas, Z.; Michl, J.; Nozik, A. J.; Johnson, J. C. *J. Phys. Chem. C* **2014**, *118*, 12121.
(22) Seixas de Melo, J. S. S.; Burrows, H. D.; Serpa, C.; Arnaut, L. G. *Angew. Chem., Int. Ed.* **2007**, *46*, 2094.
(23) Johnson, J. C.; Stepp, B. R.; Ryerson, J. L.; Smith, M. B.; Akdag, A.; Michl, J., unpublished results.
(24) Weinhold, F.; Landis, C. R. *Valency and Bonding: A Natural Bond Orbital Donor-Acceptor Perspective*; Cambridge University Press: Cambridge, UK/New York, 2005.
(25) Kosower, E. M.; Poziomek, E. J. *J. Am. Chem. Soc.* **1963**, *85*, 2035.
(26) Brook, D. J. R.; Haltiwanger, R. C.; Koch, T. H. *J. Am. Chem. Soc.* **1991**, *113*, 5910.
(27) Katritzky, A. R.; Zerner, M. C.; Karelson, M. M. *J. Am. Chem. Soc.* **1986**, *108*, 7213.
(28) Viehe, H. G.; Janousek, Z.; Merényi, R.; Stella, L. *Acc. Chem. Res.* **1985**, *18*, 148.
(29) Jacquemin, D.; Perpète, E. A.; Medved', M.; Scalmani, G.; Frisch, M. J.; Kobayashi, R.; Adamo, C. *J. Chem. Phys.* **2007**, *126*, 191108.
(30) Dreuw, A.; Head-Gordon, M. *Chem. Rev.* **2005**, *105*, 4009.
(31) Frisch, M. J.; et al. *Gaussian 09*, Revision A.02; Gaussian, Inc.: Wallingford, CT, 2009. (For complete reference, see the Supporting Information).
(32) Yanai, T.; Tew, D.; Handy, N. *Chem. Phys. Lett.* **2004**, *393*, 51.
(33) Schäfer, A.; Huber, C.; Ahlrichs, R. *J. Chem. Phys.* **1994**, *100*, 5829.
(34) Andersson, K.; Malmqvist, P.-Å.; Roos, B. O.; Sadlej, A. J.; Wolinski, K. *J. Phys. Chem.* **1990**, *94*, 5483.
(35) Andersson, K.; Malmqvist, P.-Å.; Roos, B. O. *J. Chem. Phys.* **1992**, *96*, 1218.
(36) Aquilante, F.; De Vico, L.; Ferré, N.; Ghigo, G.; Malmqvist, P.-Å.; Neográy, P.; Pedersen, T. B.; Pitoňák, M.; Reiher, M.; Roos, B. O.; Serrano-Andrés, L.; Urban, M.; Veryazov, V.; Lindh, R. *J. Comput. Chem.* **2010**, *31*, 224.
(37) Veryazov, V.; Widmark, P. O.; Serrano-Andrés, L.; Lindh, R.; Roos, B. O. *Int. J. Quantum Chem.* **2004**, *100*, 626.
(38) Karlström, G.; Lindh, R.; Malmqvist, P.-Å.; Roos, B. O.; Ryde, U.; Veryazov, V.; Widmark, P.-O.; Cossi, M.; Schimmelpfennig, B.; Neográy, P.; Seijo, N. *Comput. Mater. Sci.* **2003**, *28*, 222.
(39) Pierloot, K.; Dumez, B.; Widmark, P.-O.; Roos, B. O. *Theor. Chim. Acta* **1995**, *90*, 87.
(40) Widmark, P.-O.; Malmqvist, P.-Å.; Roos, B. O. *Theor. Chim. Acta* **1990**, *77*, 291.
(41) Widmark, P.-O.; Persson, B. J.; Roos, B. O. *Theor. Chim. Acta* **1991**, *79*, 419.
(42) Barone, V.; Cossi, M. *J. Phys. Chem. A* **1998**, *102*, 1995.
(43) Cossi, M.; Rega, N.; Scalmani, G.; Barone, V. *J. Chem. Phys.* **2001**, *114*, 5691.